

Price-based strategies for mitigating electric vehicle-induced overloads on distribution systems

F. Li, I. Kocar, A. Lesage-Landry

G-2023-48

October 2023

La collection *Les Cahiers du GERAD* est constituée des travaux de recherche menés par nos membres. La plupart de ces documents de travail a été soumis à des revues avec comité de révision. Lorsqu'un document est accepté et publié, le pdf original est retiré si c'est nécessaire et un lien vers l'article publié est ajouté.

Citation suggérée : F. Li, I. Kocar, A. Lesage-Landry (Octobre 2023). Price-based strategies for mitigating electric vehicle-induced overloads on distribution systems, Rapport technique, Les Cahiers du GERAD G- 2023-48, GERAD, HEC Montréal, Canada.

Avant de citer ce rapport technique, veuillez visiter notre site Web (<https://www.gerad.ca/fr/papers/G-2023-48>) afin de mettre à jour vos données de référence, s'il a été publié dans une revue scientifique.

The series *Les Cahiers du GERAD* consists of working papers carried out by our members. Most of these pre-prints have been submitted to peer-reviewed journals. When accepted and published, if necessary, the original pdf is removed and a link to the published article is added.

Suggested citation: F. Li, I. Kocar, A. Lesage-Landry (October 2023). Price-based strategies for mitigating electric vehicle-induced overloads on distribution systems, Technical report, Les Cahiers du GERAD G-2023-48, GERAD, HEC Montréal, Canada.

Before citing this technical report, please visit our website (<https://www.gerad.ca/en/papers/G-2023-48>) to update your reference data, if it has been published in a scientific journal.

La publication de ces rapports de recherche est rendue possible grâce au soutien de HEC Montréal, Polytechnique Montréal, Université McGill, Université du Québec à Montréal, ainsi que du Fonds de recherche du Québec – Nature et technologies.

Dépôt légal – Bibliothèque et Archives nationales du Québec, 2023
– Bibliothèque et Archives Canada, 2023

The publication of these research reports is made possible thanks to the support of HEC Montréal, Polytechnique Montréal, McGill University, Université du Québec à Montréal, as well as the Fonds de recherche du Québec – Nature et technologies.

Legal deposit – Bibliothèque et Archives nationales du Québec, 2023
– Library and Archives Canada, 2023

Price-based strategies for mitigating electric vehicle-induced overloads on distribution systems

Feng Li ^{a, b, d}

Ilhan Kocar ^c

Antoine Lesage-Landry ^{a, b}

^a GERAD, Montréal (Qc), Canada, H3T 1J4

^b Département de Génie Électrique, Polytechnique Montréal, Montréal (Qc), Canada, H3C 3A7

^c Department of Electrical Engineering, Hong Kong Polytechnic University, Hong Kong SAR, China

^d CYME International T&D, Brossard (Qc), Canada J4Z 0N5

feng.li@polymtl.ca

ilhan.kocar@polyu.edu.hk

antoine.lesage-landry@polymtl.ca

October 2023
Les Cahiers du GERAD
G–2023–48

Copyright © 2023 GERAD, Li, Kocar, Lesage-Landry, IEEE. This paper is a preprint (IEEE “submitted” status). Personal use of this material is permitted. Permission from IEEE must be obtained for all other uses, in any current or future media, including reprinting/republishing this material for advertising or promotional purposes, creating new collective works, for resale or redistribution to servers or lists, or reuse of any copyrighted component of this work in other works.

Les textes publiés dans la série des rapports de recherche *Les Cahiers du GERAD* n'engagent que la responsabilité de leurs auteurs. Les auteurs conservent leur droit d'auteur et leurs droits moraux sur leurs publications et les utilisateurs s'engagent à reconnaître et respecter les exigences légales associées à ces droits. Ainsi, les utilisateurs:

- Peuvent télécharger et imprimer une copie de toute publication du portail public aux fins d'étude ou de recherche privée;
- Ne peuvent pas distribuer le matériel ou l'utiliser pour une activité à but lucratif ou pour un gain commercial;
- Peuvent distribuer gratuitement l'URL identifiant la publication.

Si vous pensez que ce document enfreint le droit d'auteur, contactez-nous en fournissant des détails. Nous supprimerons immédiatement l'accès au travail et enquêterons sur votre demande.

The authors are exclusively responsible for the content of their research papers published in the series *Les Cahiers du GERAD*. Copyright and moral rights for the publications are retained by the authors and the users must commit themselves to recognize and abide the legal requirements associated with these rights. Thus, users:

- May download and print one copy of any publication from the public portal for the purpose of private study or research;
- May not further distribute the material or use it for any profit-making activity or commercial gain;
- May freely distribute the URL identifying the publication.

If you believe that this document breaches copyright please contact us providing details, and we will remove access to the work immediately and investigate your claim.

Abstract : This paper first introduces a computationally efficient approach for conducting a time-series impact analysis of electric vehicle (EV) charging on the loading levels of power system equipment. This study incorporates the stochastic nature of EV owners' charging behaviours by modelling various charging profiles as probability distributions. This work then develops new mitigation strategies to temporally shift EV charging from periods of equipment overloading to alternative time periods to improve power system equipment lifetime. A reward program and a time-of-use (TOU) tariff are proposed to incentivize EV owners to participate to the mitigation effort. A search algorithm integrating a convex optimization problem is developed to determine optimal incentive levels and quantify resulting changes in EV owner charging behaviours. The proposed mitigation strategies are numerically evaluated on a modified version of the large-scale IEEE-8500 test feeder with a high EV penetration to mitigate the overloading of the substation transformer.

Keywords: Electric vehicles, power distribution networks, equipment overload, demand response, convex program.

Acknowledgements: This work was funded by Eaton Corporation and Natural Sciences and Engineering Research Council of Canada (NSERC).

1 Introduction

As the electrification of the transportation sector promotes the adoption of electric vehicles (EVs), the penetration of EVs is rapidly increasing in distribution systems. While EVs offer the advantage of reducing reliance on fossil fuels and lowering greenhouse gas emissions, charging them can pose significant challenges to power distribution networks, especially in scenarios with high EV penetration. Abnormal operating conditions may occur such as equipment overloading, voltage fluctuations, phase imbalances, harmonic distortions, and more [3, 14]. From the perspective of utilities, stochastic analyses are necessary to study the impact that EV charging may have on the network conditions. These analyses consider the uncertainties in EV charging-related variables, e.g., locations, start time, duration, and power levels, and help reveal potential abnormal conditions on power networks [12, 17, 20]. It is important to address the identified network issues through mitigation plans and network optimization to ensure safe grid operations and maintain high-quality service.

A conventional approach to mitigate these issues requires substantial infrastructure investments, including expanding equipment capacity and deploying voltage regulation and reactive power control technologies [4, 11]. Alternatively, optimal charging schedule for EVs connected to the network can be derived through coordination to minimize network losses [7, 26], reduce the peak demand [22], and limit transformers' loading [21]. However, how incentive plans can be designed to attract customers to participate in coordinated charging is not discussed in these works. Demand response (DR) programs, on the other hand, provide a potential solution to the challenges posed by EV charging. These programs, either incentive-based [24] or price-based [5, 25], are designed to shift EV charging loads to periods when the grids are lightly loaded. For example, in [24] an incentive-based DR program is proposed to minimize impacts of controllable loads to distribution networks. A constrained optimization problem is formulated to allocate a demand limit for each customer during a time period, and customers can select charging hours for their EVs as long as the demand limit is respected at all times. Effectiveness of the DR program is shown at different EV penetration levels; however, the relationship between the incentive and the demand limit is not clear. In [25], load patterns are studied when a DR strategy is implemented to non-critical loads (including EV charging) with time-of-use (TOU) rates. In [5], to reduce EV charging demand at the peak hours, a schedule is developed in response to the TOU rates to minimize users' charging costs. In both works, TOU rates are assumed to be pre-defined but not optimized considering variations of load demands which includes EVs.

A common shortcoming of all the aforementioned works is that the proposed strategies are not demonstrated on large-scale networks for effectiveness. This could be due to the heavy computation burden when assessing the network conditions under the strategies for a large number of EVs while accounting for charging behaviour uncertainties. In our previous works [20], we have proposed a rapid estimation method to perform a stochastic analysis for impacts of EV charging on distribution networks. In this work, we focus on the impacts of EV charging to loading levels of key network equipment, e.g., a substation transformer during a period of time. As severe overloading may shorten equipment's service lifetime and cause premature failures [8], we propose an approach to avoid loss of equipment's lifetime by mitigating overloading issues identified by the stochastic impact analysis.

Key contributions of the paper include:

- Proposing incentive-based mitigation strategies that aim to shift EV charging from the peak period when equipment is heavily loaded, to the off-peak period when the equipment is lightly loaded. Two types of incentive programs are considered under the proposed mitigation strategies: reward for reducing power consumption during the peak period and a TOU tariff.
- Formulating a bi-level optimization problem to design the mitigation strategy. The problem is then reformulated into a computationally tractable single-level convex program.
- Embedding the convex program into a novel search algorithm to efficiently determine optimal incentive levels and the corresponding shift in customer charging probabilities. The proof of convergence is provided and the optimality of the converged value is discussed.

The inclusion of a TOU tariff, the analysis of the convex reformulation, and the novel search algorithm along with the convergence proof are major enhancements to [19].

The rest of the paper is organized as follows: Section 2 presents the model for time-series stochastic impact analysis in terms of EV penetration rate. In Section 3, we derive a bi-level optimization problem to design the mitigation strategy. Instead of directly solving the non-linear optimization problem, in Section 4 we reformulate it to a convex problem, and embed it into a search algorithm to determine the reward level and the TOU tariff. Section 5 illustrates the results of the proposed mitigation strategy to an overloaded substation transformer due to EV charging on a modified IEEE-8500 test feeder. Finally, we conclude in Section 6 and point out some future work directions.

2 Time-series stochastic EV impact analysis

In our previous work [20], we developed a rapid estimation method (REM) to analyze the impact of grid-edge technologies, including EVs to distribution networks at a specific time, e.g., loading levels of power system equipment during peak hours, under various penetration rates. Due to its computational efficiency, we extend the method here to perform a time-series impact analysis of EV charging to distribution networks.

2.1 Assumption on input data

We assume that the following input data for the analysis is given, which can be gathered from either statistical surveys such as [6, 23, 28] or can be estimated from EV usage and travel data [13].

- A set of L charging profiles $\mathcal{L}_{\text{EV}} = \{l_{\text{EV}}^j(t)\}_{j=1,2,\dots,L}$, where $l_{\text{EV}}^j(t)$ is an EV charging profile in kW during an entire day discretized over the set $\mathcal{T} = \{1, 2, \dots, T\}$. Here, T is the cardinality of \mathcal{T} and depends on the time step, e.g., $T = 96$ if each time step has a duration of $\Delta t = 15$ minutes. For a profile, if charging is active at t , $l_{\text{EV}}^j(t) > 0$ and $l_{\text{EV}}^j(t) = 0$ otherwise.
- Adoption probability $\text{Pr}^i[\mathcal{L}_{\text{EV}}] \in \mathbb{R}^L$ attached to customer $i \in \{1, 2, \dots, N_m\}$ to adopt a charging profile type j in \mathcal{L}_{EV} , where N_m is the total number of customers.

Note that we do not presume any type of distribution for $\text{Pr}^i(\mathcal{L}_{\text{EV}})$, hence it can be of any arbitrary probability distribution. In addition, the network model for the impact analysis should also be available such that equipment data and network topology can be extracted. Finally, we consider only the residential customers in this paper as they account for up to 80% of charging events with diversified and stochastic charging patterns [27], but our approach can be extended to other customer types without limitations as long as corresponding charging profiles and adoption probabilities are provided.

2.2 Equipment loading levels

Denote $x_t(p) \in \mathbb{R}^T$ as the loading levels of an equipment (in per-unit or percentage) on the power distribution network for $t \in \mathcal{T}$ at an EV penetration rate p . The penetration rate is defined as the ratio of the total number of EVs n_{EV} over the total number of customers on the network N_m , i.e., $p = n_{\text{EV}}/N_m$. Due to the stochasticity of EV charging events, x_t is no longer deterministic; rather, it should be characterized by its probability density function (PDF) at p , which is denoted by $m(x_t, p)$. The evolution of $m(x_t, p)$ with respect to p can be described by the following Fokker-Planck equation (FPE):

$$\frac{\partial m(x_t, p)}{\partial p} + \frac{\partial}{\partial x_t} \left\{ m(x_t, p) u(x_t, p) \right\} = d \frac{\partial^2 m(x_t, p)}{\partial x_t^2}, \quad (1)$$

subject to $m_0 = m(x_t, p^0)$. Without loss of generality, let us assume $p^0 = 0$ hereinafter, i.e., the baseline network does not have any EV. In (1), the diffusion velocity term d is a small positive constant, and the drift velocity term $u(x_t, p)$ specifies the rate of change to equipment loading level x_t at a given p due to EV charging.

The term $u(x_t, p)$ is computed by taking the derivative of equipment loading levels at given p . For distribution networks, $u(x_t, p)$ is usually computed by-phase because the equipment loading level is calculated on each phase. However, for the purpose of this paper the REM is modified to compute the loading level of the equipment on all connected phases. Let $x_{t,e}(p)$ be the loading level of equipment e at EV penetration p , and $x_{t,e}(p)$ can be expressed by:

$$x_{t,e}(p) = x_{t,e}(p^0) + g_{t,e}(p), \quad (2)$$

where $x_{t,e}(p^0)$ is the loading level of e which can be obtained from a power flow analysis to the baseline network when no EV is connected, and $g_{t,e}(p)$ is the increased amount of loading to e . We can approximate $g_{t,e}(p)$ by the following [20]:

$$g_{t,e}(p) \approx \frac{n_{\text{EV}} \Pr_e(p) \mathbb{E}[S_{\text{EV}}](t)}{S_e}, \quad (3)$$

where $\Pr_e(p)$ is the time-invariant probability that EVs are connected to sections downstream of e , $\mathbb{E}[S_{\text{EV}}](t) \in \mathbb{R}$ is the expected apparent power at time t of an EV being charged at downstream of e which is independent of p , and $S_e \in \mathbb{R}$ is the rated power of e which is assumed to be known. Readers are referred to [20] for more details on the calculation of $\Pr_e(p)$. The drift velocity $u(x_{t,e}, p)$ can then be computed for each $t \in \mathcal{T}$ by taking the derivative of $x_{t,e}(p)$ or equivalently of $g_{t,e}(p)$ with respect to p .

Once $u(x_{t,e}, p)$ is computed, (1) is numerically solved by the finite-volume method (FVM) using an implicit scheme [18] for a given t . Thus, we obtain a sequence of PDFs indexed by p , from which the mean or any percentile value of $x_{t,e}(p)$ can be computed as well as the probability of e being overloaded at t . To evaluate equipment loading levels for period \mathcal{T} , the analysis must be repeated for each $t \in \mathcal{T}$. As the result obtained at time t does not depend on that at any other t , the process can be parallelized for improved efficiency. The application of REM for such a time-series analysis is denoted as the ts-REM hereinafter. If the ts-REM results indicate that the equipment is frequently overloaded or the overload lasts long at certain EV penetration rate, a higher risk of premature equipment failure is expected which in turn increases the operating and maintenance costs for utilities. Given the increasing EV penetration, a mitigation strategy becomes necessary to manage equipment loading levels.

3 Mitigation strategy

The expected charging power $\mathbb{E}[S_{\text{EV}}]$ of an EV connected downstream of equipment e in (3) is expressed by:

$$\begin{aligned} \mathbb{E}[S_{\text{EV}}](t) &= \frac{1}{|\mathcal{K}_e|} \sum_{i \in \mathcal{K}_e} \mathbb{E}[S_{\text{EV}}^i](t) \\ \mathbb{E}[S_{\text{EV}}^i](t) &= \sum_j l_{\text{EV}}^j(t) \Pr_{\mathcal{L}}^i[j], \end{aligned} \quad (4)$$

where \mathcal{K}_e is the set of customers who are downstream of e , and $|\mathcal{K}_e|$ is its cardinality. If all customers on the network are downstream of e , then $|\mathcal{K}_e| = N_m$. If EV owning customers tend to charge their vehicles during peak hours (denoted by \mathcal{T}^{P}) when the total demand is already high, these customers possess high probabilities of adopting charging profiles that are active during \mathcal{T}^{P} (denoted by $\mathcal{L}_{\text{EV}}^{\text{P}}$). In such a case, it is expected that $\mathbb{E}[S_{\text{EV}}](t)$ is large for $t \in \mathcal{T}^{\text{P}}$. Consequently, the extra loading due to EV charging will be significant according to (3). The probability of overloading network equipment is then greatly increased, especially when p is high. Conversely, if a control mechanism is in place to limit $\mathbb{E}[S_{\text{EV}}]$ during \mathcal{T}^{P} , the equipment overloading can be mitigated.

Considering (4), $\mathbb{E}[S_{\text{EV}}]$ during \mathcal{T}^{P} can be reduced if the probabilities $\Pr_{\mathcal{L}}^i[j \in \mathcal{L}_{\text{EV}}^{\text{P}}]$ of all customers are decreased while those in $\Pr_{\mathcal{L}}^i[j \in \mathcal{L}_{\text{EV}} \setminus \mathcal{L}_{\text{EV}}^{\text{P}}]$ are increased. In other words, we are shifting high values of $\mathbb{E}[S_{\text{EV}}]$ during \mathcal{T}^{P} to other time periods. Under such a strategy, we can mitigate potential

overloading issues to network equipment due to EV charging during \mathcal{T}^P by reducing customers' probabilities of charging their EVs in this period. In the following section, we discuss how modifications to $\Pr_{\mathcal{L}}^i$ are made when customer i participates in a mitigation strategy.

3.1 Modification to charging profile probabilities

We partition the time period \mathcal{T} and the set of profile types \mathcal{L}_{EV} into the following disjoint sets:

$$\begin{aligned}\mathcal{T} &= \mathcal{T}^P \cup \mathcal{T}^{\text{OP}} \cup \mathcal{T}^{\text{MP}} \\ \mathcal{L}_{\text{EV}} &= \mathcal{L}_{\text{EV}}^P \cup \mathcal{L}_{\text{EV}}^{\text{OP}} \cup \mathcal{L}_{\text{EV}}^{\text{MP}},\end{aligned}\tag{5}$$

where

\mathcal{T}^P is the peak period and $\mathcal{L}_{\text{EV}}^P$ is the set of profiles where charging starts during \mathcal{T}^P . Under a mitigation strategy, customers' probabilities $\Pr_{\mathcal{L}}^i[j \in \mathcal{L}_{\text{EV}}^P]$ are to be reduced;

\mathcal{T}^{OP} is the off-peak period and $\mathcal{L}_{\text{EV}}^{\text{OP}}$ is the set of profiles where charging starts during \mathcal{T}^{OP} , and customers' probabilities $\Pr_{\mathcal{L}}^i[j \in \mathcal{L}_{\text{EV}}^{\text{OP}}]$ are to be increased under a mitigation strategy, and;

\mathcal{T}^{MP} is the mid-peak period and $\mathcal{L}_{\text{EV}}^{\text{MP}}$ is the set of profiles where charging starts during \mathcal{T}^{MP} , and under a mitigation strategy customers' probabilities $\Pr_{\mathcal{L}}^i[j \in \mathcal{L}_{\text{EV}}^{\text{MP}}]$ remain unchanged.

In general, \mathcal{T}^P should include the hours during which the network is heavily-loaded, hence we can assume that overloading never occurs to equipment during \mathcal{T}^{OP} and \mathcal{T}^{MP} periods, even when a mitigation strategy is applied.

Let $\mathbf{y}^P \in \{0, 1\}^L = [y_j^P, j = 1, 2, \dots, L]^\top$ be an indicator vector where $y_j^P = 1$ if $j \in \mathcal{L}_{\text{EV}}^P$ and $y_j^P = 0$ otherwise. Similarly, let $\mathbf{y}^{\text{OP}} \in \{0, 1\}^L$ be another indicator vector for profiles in $\mathcal{L}_{\text{EV}}^{\text{OP}}$. For a given $\Pr_{\mathcal{L}}^i$, we have $\Pr_{\mathcal{L}}^i = \Pr_{\mathcal{L}}^{i,P} + \Pr_{\mathcal{L}}^{i,\text{OP}} + \Pr_{\mathcal{L}}^{i,\text{MP}}$, where $\Pr_{\mathcal{L}}^{i,P} = \Pr_{\mathcal{L}}^i \odot \mathbf{y}^P$, $\Pr_{\mathcal{L}}^{i,\text{OP}} = \Pr_{\mathcal{L}}^i \odot \mathbf{y}^{\text{OP}}$, and \odot is the Hadamard product.

Denote $\Sigma^{i,P} = (\Pr_{\mathcal{L}}^i)^\top \mathbf{y}^P \in [0, 1]$ as customer i 's total probability of adopting charging profiles in $\mathcal{L}_{\text{EV}}^P$. Suppose that we would like to reduce $\Sigma^{i,P}$ by an amount $\Delta_{\text{prob}}^i \geq 0$, such that the customer's probabilities of adopting charging profiles in $\mathcal{L}_{\text{EV}}^P$ are reduced. Let $\widetilde{\Pr}_{\mathcal{L}}^{i,P} \in [0, 1]$ be the resulting probabilities, and we have:

$$\widetilde{\Pr}_{\mathcal{L}}^{i,P} = \Pr_{\mathcal{L}}^{i,P} - \frac{\Delta_{\text{prob}}^i}{\Sigma^{i,P}} \Pr_{\mathcal{L}}^{i,P}.\tag{6}$$

We consider (6) as equivalent to scaling down the probabilities in $\Pr_{\mathcal{L}}^{i,P}$ such that the sum of reductions adds up to Δ_{prob}^i . To ensure that all elements of $\widetilde{\Pr}_{\mathcal{L}}^{i,P}$ are non-negative, we impose $0 \leq \Delta_{\text{prob}}^i \leq \Sigma^{i,P}$. Conversely, we scale up the probabilities in $\Pr_{\mathcal{L}}^{i,\text{OP}}$ such that the total probability is increased by Δ_{prob}^i , i.e.,

$$\widetilde{\Pr}_{\mathcal{L}}^{i,\text{OP}} = \Pr_{\mathcal{L}}^{i,\text{OP}} + \frac{\Delta_{\text{prob}}^i}{\Sigma^{i,\text{OP}}} \Pr_{\mathcal{L}}^{i,\text{OP}},\tag{7}$$

where $\Sigma^{i,\text{OP}} = (\Pr_{\mathcal{L}}^i)^\top \mathbf{y}^{\text{OP}} \in [0, 1]$. From (6) and (7), the resulting probability distribution $\widetilde{\Pr}_{\mathcal{L}}^i$ obtained by shifting probabilities of charging during \mathcal{T}^P to \mathcal{T}^{OP} can be expressed by:

$$\widetilde{\Pr}_{\mathcal{L}}^i = \widetilde{\Pr}_{\mathcal{L}}^{i,P} + \widetilde{\Pr}_{\mathcal{L}}^{i,\text{OP}} + \Pr_{\mathcal{L}}^{i,\text{MP}}.\tag{8}$$

To acknowledge the fact that not all customers are willing to change their charging habits under a mitigation program, we let $\mathcal{K}_p \subseteq \mathcal{K}_e$ be the set of customers who participate, and $\lambda_p \in [0, 1]$ be the participation factor, which is defined by $\lambda_p = \frac{|\mathcal{K}_p|}{|\mathcal{K}_e|}$. We have:

$$\Delta_{\text{prob}}^i = 0, \quad \forall i \in \mathcal{K}_e \setminus \mathcal{K}_p.\tag{9}$$

We extend the above process of modifying charging profile probabilities to all customers in a matrix form. By denoting $\mathbf{Pr}_{\mathcal{L}} \in [0, 1]^{|\mathcal{K}_e| \times L}$ as the EV charging profile probabilities for all customers in \mathcal{K}_e , we extract the probabilities of profiles in $\mathcal{L}_{\text{EV}}^{\text{P}}$ for all customers by $\mathbf{Pr}_{\mathcal{L}}^{\text{P}} = \mathbf{Pr}_{\mathcal{L}} \mathbf{y}^{\text{P}}$, where $\mathbf{y}^{\text{P}} = \text{diag}\{\mathbf{y}^{\text{P}}\} \in \{0, 1\}^{L \times L}$. Similarly, the probabilities of profiles in $\mathcal{L}_{\text{EV}}^{\text{OP}}$ are $\mathbf{Pr}_{\mathcal{L}}^{\text{OP}} = \mathbf{Pr}_{\mathcal{L}} \mathbf{Y}^{\text{OP}}$. We write (6) in the following matrix form for all customers:

$$\widetilde{\mathbf{Pr}}_{\mathcal{L}}^{\text{P}} = \mathbf{Pr}_{\mathcal{L}}^{\text{P}} - (\boldsymbol{\Sigma}^{\text{P}})^{-1} \boldsymbol{\Delta}_{\text{prob}} \mathbf{Pr}_{\mathcal{L}}^{\text{P}}, \quad (10)$$

where $\boldsymbol{\Sigma}^{\text{P}} = \text{diag}\{\boldsymbol{\Sigma}^{i,\text{P}}\}$ and $\boldsymbol{\Delta}_{\text{prob}} = \text{diag}\{\Delta_{\text{prob}}^i\}$ which are $|\mathcal{K}_e| \times |\mathcal{K}_e|$ square matrices. Similarly, the adjusted probabilities for profiles in $\mathcal{L}_{\text{EV}}^{\text{OP}}$ after adding $\boldsymbol{\Delta}_{\text{prob}}$ are:

$$\widetilde{\mathbf{Pr}}_{\mathcal{L}}^{\text{OP}} = \mathbf{Pr}_{\mathcal{L}}^{\text{OP}} + (\boldsymbol{\Sigma}^{\text{OP}})^{-1} \boldsymbol{\Delta}_{\text{prob}} \mathbf{Pr}_{\mathcal{L}}^{\text{OP}}. \quad (11)$$

From (10) and (11), we obtain the modified probabilities of charging profiles for all customers as,

$$\begin{aligned} \widetilde{\mathbf{Pr}}_{\mathcal{L}} &= \widetilde{\mathbf{Pr}}_{\mathcal{L}}^{\text{P}} + \widetilde{\mathbf{Pr}}_{\mathcal{L}}^{\text{OP}} + \mathbf{Pr}_{\mathcal{L}}^{\text{MP}} \\ &= \mathbf{Pr}_{\mathcal{L}}^{\text{P}} - (\boldsymbol{\Sigma}^{\text{P}})^{-1} \boldsymbol{\Delta}_{\text{prob}} \mathbf{Pr}_{\mathcal{L}}^{\text{P}} \\ &\quad + \mathbf{Pr}_{\mathcal{L}}^{\text{OP}} + (\boldsymbol{\Sigma}^{\text{OP}})^{-1} \boldsymbol{\Delta}_{\text{prob}} \mathbf{Pr}_{\mathcal{L}}^{\text{OP}} + \mathbf{Pr}_{\mathcal{L}}^{\text{MP}} \\ &= \mathbf{Pr}_{\mathcal{L}} - \boldsymbol{\Sigma}_{\text{inv}} \begin{bmatrix} \boldsymbol{\Delta}_{\text{prob}} \mathbf{Pr}_{\mathcal{L}} & \mathbf{0}_{|\mathcal{K}_e|,L} \\ \mathbf{0}_{|\mathcal{K}_e|,L} & \boldsymbol{\Delta}_{\text{prob}} \mathbf{Pr}_{\mathcal{L}} \end{bmatrix} \mathbf{y}, \end{aligned} \quad (12)$$

where $\boldsymbol{\Sigma}_{\text{inv}} = [(\boldsymbol{\Sigma}^{\text{P}})^{-1} \quad -(\boldsymbol{\Sigma}^{\text{OP}})^{-1}] \in \mathbb{R}^{|\mathcal{K}_e| \times 2|\mathcal{K}_e|}$, $\mathbf{0}_{|\mathcal{K}_e|,L}$ is a zero-matrix, and $\mathbf{y} = [\mathbf{Y}^{\text{P}} \quad \mathbf{Y}^{\text{OP}}]^{\text{T}} \in \{0, 1\}^{2L \times L}$.

It is remarked that (12) formulates how the probabilities are modified assuming $\boldsymbol{\Delta}_{\text{prob}}$ is given. Recall that for a non-participating customer $i \notin \mathcal{K}_p$, $\Delta_{\text{prob}}^i = 0$. For each participating customer, we discuss in the next section how to determine Δ_{prob}^i from an optimization problem. Without loss of generality, for the rest of the paper we assume that $\lambda_p = 1$, i.e., all customers are participating into the mitigation program.

3.2 Optimal values of $\boldsymbol{\Delta}_{\text{prob}}$

Recall that the goal of encouraging EV owners to shift their probabilities of charging periods from \mathcal{T}^{P} to \mathcal{T}^{OP} is to avoid overloading the key network equipment, which might shorten equipment lifetime. Thus, optimal values of $\boldsymbol{\Delta}_{\text{prob}}$ should meet the following conditions: (a) no extensive overloading occurs to the equipment and its nominal lifetime is maintained and; (b) customers are driven by incentives to adopt charging behaviours according to the adjusted $\widetilde{\mathbf{Pr}}_{\mathcal{L}}$ which does not result in unmotivated costs to utilities.

3.2.1 Impact of overloading on equipment lifetime and cost

As overloading often results in higher operating temperature of the equipment, its expected lifetime is reduced if the equipment is periodically overheated due to the loading levels [9]. To assess the reduced lifetime, thermal-aging models are used. For example, IEEE standard C57.91 [2] describes the thermal-aging model for transformers and IEEE standard 1283-2013 [1] describes the model for lines and conductors. Details on the thermal-aging model are omitted due to the space limit, but let us denote TAM : *loading* $\mapsto F_{\text{life}}$ as the thermal-aging model. Here, *loading* $\in \mathbb{R}^T$ is the equipment loading levels over the period \mathcal{T} , and F_{life} is an annualized stress factor indicating the ratio of the expected over the nominal lifetime of the equipment. If $F_{\text{life}} = 1$, the equipment's expected lifetime is maintained at its nominal value, whereas the equipment is stressed by the loading levels and the lifetime is reduced when $F_{\text{life}} > 1$.

Let $c(F_{\text{life}})$ denote the increased annual cost of the equipment (depreciation, operating & maintenance, etc.) due to the shortened lifetime, i.e.,

$$c(F_{\text{life}}) = c_{\text{annual}}(\max\{1, F_{\text{life}}\} - 1), \quad (13)$$

where $c_{\text{annual}} > 0$ is the total annual cost at the nominal lifetime. We remark that it is possible to have $F_{\text{life}} < 1$. This indicates that the equipment is still in service after its nominal lifetime is reached. However, in this paper, we assume that no equipment operates beyond its nominal lifetime for economical and safety reasons. Hence, when $F_{\text{life}} \leq 1$, there is no saving in cost and we have $c(F_{\text{life}} \leq 1) = 0$.

3.2.2 Incentives to customers

Recall that incentives are given to customers in exchange for changes in their charging habits, i.e., adjusting $\mathbf{Pr}_{\mathcal{L}}$ to $\widetilde{\mathbf{Pr}}_{\mathcal{L}}$ by reducing Δ_{prob} from their total probabilities of charging EVs during \mathcal{T}^{P} . Let $R^i(\Delta_{\text{prob}}^i)$ denote the annualized incentive given to customer i , and $\widetilde{F}_{\text{life}}$ the resulting lifetime factor when all customers are adopting $\widetilde{\mathbf{Pr}}_{\mathcal{L}}$. The total annual incentives given to all customers should not exceed $c(F_{\text{life}}) - c(\widetilde{F}_{\text{life}})$; otherwise, the best option for the utility is to keep operating the equipment at a reduced lifetime F_{life} and to pay no incentives to customers. Hence, $c(F_{\text{life}}) - c(\widetilde{F}_{\text{life}})$ is considered as a “budget” for the total incentives, and we have the following constraint on the total incentives to be paid:

$$\sum_{i=1}^{|\mathcal{K}_e|} R^i \leq c(F_{\text{life}}) - c(\widetilde{F}_{\text{life}}). \quad (14)$$

It is remarked that if $c(F_{\text{life}}) = 0$, it is not necessary to adjust customers’ charging habits hence no incentive is given to customers and $\Delta_{\text{prob}} = 0$. For the rest of paper, we assume that $F_{\text{life}} > 1$ initially with EVs connected to the network before any mitigation strategy is adopted, hence $c(F_{\text{life}}) > 0$.

In this work, two types of incentives are considered: (1) reward for reduced consumption of EV charging during \mathcal{T}^{P} , and (2) time-of-use (TOU) pricing during the entire day. The formulation as well as the objective function of each type of incentive is detailed in the following sections. It is assumed here that the reward or TOU pricing applies only to EV consumption, i.e., a separate meter is installed for the EV charger [10].

Reward for reduced consumption of EV charging during \mathcal{T}^{P} As each customer contributes to reducing equipment loading during \mathcal{T}^{P} , a reward is given based on the expected reduction of consumption for EV charging. Customer i ’s daily reward is given by:

$$R_{\text{day}}^{i,\text{reward}} = r \sum_{t \in \mathcal{T}^{\text{P}}} \Delta E^i \quad (15)$$

$$\Delta E^i = \Delta t \sum_j l_{\text{EV}}^j(t) \left(\text{Pr}_{\mathcal{L}}^i(j) - \widetilde{\text{Pr}}_{\mathcal{L}}^i(j) \right), \quad (16)$$

where Δt is the time step, and $r \in \mathbb{R}$ (\$/kWh) is the unit reward applicable to all customers which is another variable in the optimization problem. The annualized reward for customer i is:

$$R^i = 365 R_{\text{day}}^{i,\text{reward}}. \quad (17)$$

In addition, the following constraint is imposed which ensures that each customer’s total expected energy consumed for EV charging remains unchanged with and without the reward.

$$\sum_{t \in \mathcal{T}} \Delta E^i = 0, \quad \forall i = 1, 2, \dots, |\mathcal{K}_e|. \quad (18)$$

TOU pricing Given that we have partitioned each day into three periods, the electricity rate needs to be determined for each period. Let $p_{\text{rate}}^{\text{nom}}$ (\$/kWh) be the nominal rate. Because customers’ charging

probabilities in the mid-peak period \mathcal{T}^{MP} remain unchanged, the rate remains at $p_{\text{rate}}^{\text{nom}}$, i.e., $p_{\text{rate}}^{\text{MP}} = p_{\text{rate}}^{\text{nom}}$. For the off-peak period, the rate is decreased by $\xi \geq 0$, i.e., $p_{\text{rate}}^{\text{OP}} = p_{\text{rate}}^{\text{nom}} - \xi$. For the peak period, a surcharge $\eta \geq 0$ is added to the nominal rate, i.e., $p_{\text{rate}}^{\text{P}} = p_{\text{rate}}^{\text{nom}} + \eta$. Both ξ and η are to be determined by the optimization problem. Under such a TOU pricing, customer i 's daily savings in electricity price is:

$$R_{\text{day}}^{i,\text{TOU}} = (p_{\text{rate}}^{\text{nom}} + \eta) \sum_{t \in \mathcal{T}^{\text{P}}} \Delta E^i + (p_{\text{rate}}^{\text{nom}} - \xi) \sum_{t \in \mathcal{T}^{\text{OP}}} \Delta E^i - \eta \sum_{t \in \mathcal{T}^{\text{P}}} E^i + \xi \sum_{t \in \mathcal{T}^{\text{OP}}} E^i + p_{\text{rate}}^{\text{nom}} \sum_{t \in \mathcal{T}^{\text{MP}}} \Delta E^i, \quad (19)$$

where $E^i = \Delta t \sum_j l_{\text{EV}}^j(t) \text{Pr}_{\mathcal{L}}^i(j)$ and ΔE^i is defined in (16). The annualized reward for customer i is:

$$R^i = 365 R_{\text{day}}^{i,\text{TOU}}. \quad (20)$$

The EV charging energy conservation constraint (18) also applies. Further, because neither the electricity price during the off-peak period nor each customer's reward can be negative, the following constraints are added:

$$\begin{aligned} p_{\text{rate}}^{\text{OP}} &> 0 \\ R_{\text{day}}^{i,\text{TOU}} &> 0. \end{aligned} \quad (21)$$

3.2.3 Optimization problem formulation

The optimization problem is formulated to identify optimal levels of Δ_{prob} and incentives such that utilities' costs are minimized while the equipment is maintained at its nominal lifetime or as close as possible. This is expressed as:

$$\begin{aligned} \min_{\Delta_{\text{prob}}, r, (\xi, \eta)} \quad & \sum_{i=1}^{|\mathcal{K}_e|} R^i \\ \text{subject to} \quad & \Delta_{\text{prob}} \in \arg \min_{\Delta_{\text{prob}}} |\tilde{F}_{\text{life}} - 1| \\ & \text{subject to } 0 \leq \Delta_{\text{prob}} \leq \Sigma^{\text{P}} \\ & \text{loading} = \text{ts-REM}(\tilde{\mathbf{Pr}}_{\mathcal{L}}) \\ & \tilde{F}_{\text{life}} = \text{TAM}(\text{loading}) \\ & (9), (12), (13), (14), (18), \text{ and} \\ & (15) \text{ or } (19), (21). \end{aligned} \quad (22)$$

Recall that ts-REM refers to the time-series REM method presented in Section 2 which evaluates impacts of $\tilde{\mathbf{Pr}}_{\mathcal{L}}$ to the equipment loading levels *loading*, and TAM refers to the thermal-aging model which computes the lifetime factor under the resulting *loading*. Each customer's incentive can either be a reward-based as in (17) or a TOU pricing-based as in (20). If the latter is adopted, the variable r is replaced by ξ and η in (22).

4 Convex reformulation

We remark that the optimization problem formulated so far is a bi-level, non-linear, and non-convex problem, which is difficult to solve and global optimality is not guaranteed. In this section, we aim to reformulate (22) into a single-level convex optimization problem, which can be efficiently solved.

4.1 Approximation of total incentives

The total annualized reward R^i used in (14) and (22) is non-convex due to the form of $R_{\text{day}}^{i,\text{reward}}$ and $R_{\text{day}}^{i,\text{TOU}}$ in (15) and (19), respectively. To approximate the incentives, we use the price elasticity model [15, 16] to measure a customer's response to the incentive offered, where

$$-\Delta E^i = \varepsilon^i \Delta p_{\text{rate}} = \bar{\varepsilon} \frac{E^i}{p_{\text{rate}}^{\text{nom}}} \Delta p_{\text{rate}}. \quad (23)$$

In (23), due to the definition of ΔE^i in (16), a negative sign is necessary to model the expected change in energy consumption for EV charging when an incentive Δp_{rate} (e.g., r in the reward program or $-\xi$ and η in the TOU pricing) is offered under the mitigation program. The individual price elasticity ε^i of customer i is related to the energy consumed E^i , the nominal electricity price $p_{\text{rate}}^{\text{nom}}$, and an averaged price elasticity factor $\bar{\varepsilon} < 0$ which applies to all customers independent of the time period. It is remarked that we ignore the changes of energy consumed in one period due to the price change in another period, hence cross elasticity factors are not considered [15]. In addition, for given $\bar{\varepsilon}$, $p_{\text{rate}}^{\text{nom}}$, and Δp_{rate} , customers with higher consumption E^i contribute more in reducing the consumption under the mitigation strategy.

We apply (23) to the two type of incentives, and obtain:

$$\hat{R}_{\text{day}}^{i,\text{reward}} = r \Delta E^{i,\text{P}} = -\varepsilon^{i,\text{P}} r^2, \quad (24)$$

$$\hat{R}_{\text{day}}^{i,\text{TOU}} = -\varepsilon^{i,\text{P}} (\eta^2 + \eta p_{\text{rate}}^{\text{nom}}) - \varepsilon^{i,\text{OP}} (\xi^2 - \xi p_{\text{rate}}^{\text{nom}}) - \eta E^{i,\text{P}} + \xi E^{i,\text{OP}} + p_{\text{rate}}^{\text{nom}} \Delta E^{i,\text{MP}}, \quad (25)$$

where $\varepsilon^{i,\text{P}} = \bar{\varepsilon} \frac{E^{i,\text{P}}}{p_{\text{rate}}^{\text{nom}}}$ and $\varepsilon^{i,\text{OP}} = \bar{\varepsilon} \frac{E^{i,\text{OP}}}{p_{\text{rate}}^{\text{nom}}}$. The total incentives are now expressed as:

$$\hat{R}^i = \begin{cases} 365 \hat{R}_{\text{day}}^{i,\text{reward}}, & \text{if reward} \\ 365 \hat{R}_{\text{day}}^{i,\text{TOU}}, & \text{if TOU.} \end{cases} \quad (26)$$

We note that for the TOU type of incentives, constraint (21) should apply to $\hat{R}_{\text{day}}^{i,\text{TOU}}$.

4.2 Constraint to loading

In the second level of (22), we aim to maintain the equipment at its nominal lifetime by adjusting equipment's *loading*. The lifetime is likely to be shortened (i.e., $\tilde{F}_{\text{life}} > 1$) when *loading* shows severe or prolonged overloading, mainly due to simultaneous EV charging during the peak hours. While it is natural to add a constraint to limit the loading levels at all time, it is difficult to find an optimal constraint as *loading* is numerically computed by the ts-REM model. Alternatively, as discussed in Section 3 and by (3), the extra loading to the equipment due to EV charging depends on $\mathbb{E}[S_{\text{EV}}]$. Hence, constraining $\mathbb{E}[S_{\text{EV}}]$ would have an equivalent effect to limiting *loading*.

Let us assume that there exists some time-varying limit \bar{S}_t for $\mathbb{E}[\tilde{S}_{\text{EV}}]$ when a mitigation strategy is applied and $|\tilde{F}_{\text{life}} - 1|$ is minimized. Under this assumption, not only can we move the ts-REM and TAM models out of (22), we can also remove the second level of (22). The optimization problem becomes:

$$\begin{aligned} \min_{\Delta_{\text{prob}}, r, (\xi, \eta)} \quad & \sum_{i=1}^{|\mathcal{K}_e|} \hat{R}^i \\ \text{subject to} \quad & 0 \leq \Delta_{\text{prob}} \leq \Sigma^{\text{P}} \\ & \mathbb{E}[\tilde{S}_{\text{EV}}](t) \leq \bar{S}_t, \quad \forall t \in \mathcal{T} \\ & \sum_{i=1}^{|\mathcal{K}_e|} \hat{R}^i \leq c(F_{\text{life}}) \\ & (9), (12), (18), \text{ and} \\ & (24) \text{ or } (25), (21) \end{aligned} \quad (27)$$

Note that as the TAM model is not embedded in the optimization problem, the $c(\tilde{F}_{\text{life}})$ term appearing in (14) cannot be evaluated. Hence we relax it by taking the initial cost of $c(F_{\text{life}})$ as the budget. Such a relaxation is exact if $\tilde{F}_{\text{life}} = 1$, i.e., the nominal lifetime is achievable under a mitigation strategy.

The reformulated optimization problem (27) is equivalent to (22), is convex, and is readily solvable to optimality but depends on \bar{S}_t . Next, we discuss how to determine \bar{S}_t .

4.3 Determination of \bar{S}_t

In this subsection, we discuss the calculation of \bar{S}_t which is essential for (27).

4.3.1 Limit for \mathcal{T}^{OP} and \mathcal{T}^{MP}

For a given EV penetration p , the loading level $x_{t,e}(p)$ for $t \in \mathcal{T}$ can be computed via (2). As we assumed that the equipment should never be overloaded during \mathcal{T}^{OP} and \mathcal{T}^{MP} , we have the following inequality:

$$\begin{aligned} x_{t,e}(p^0) + g_{t,e}(p) &\leq 1, \\ g_{t,e}(p) &\leq 1 - x_{t,e}(p^0), \quad t \in \mathcal{T}^{\text{OP}} \cup \mathcal{T}^{\text{MP}}. \end{aligned} \quad (28)$$

Substituting (3) into (28) we get,

$$\begin{aligned} \frac{n_{\text{EV}} \Pr_e(p) \mathbb{E}[S_{\text{EV}}](t)}{S_e} &\leq 1 - x_{t,e}(p^0), \\ \mathbb{E}[S_{\text{EV}}](t) &\leq \frac{S_e (1 - x_{t,e}(p^0))}{n_{\text{EV}} \Pr_e(p)}, \quad t \in \mathcal{T}^{\text{OP}} \cup \mathcal{T}^{\text{MP}}. \end{aligned} \quad (29)$$

The right-hand side of (29) is the limit for $\mathbb{E}[S_{\text{EV}}](t)$ during the off-peak and mid-peak periods which is a sufficient condition to guarantee that the equipment is not overloaded, i.e.,

$$\bar{S}_t = \frac{S_e (1 - x_{t,e}(p^0))}{n_{\text{EV}} \Pr_e(p)}, \quad t \in \mathcal{T}^{\text{OP}} \cup \mathcal{T}^{\text{MP}}. \quad (30)$$

Note that the limit expressed in (30) is time-variant and independent of customers' charging probabilities.

4.3.2 Search for limit during \mathcal{T}^{P}

While we can analytically compute the limit for the peak period by also imposing that the equipment is not overloaded, the resulting limit may be too restricting to minimize $|\tilde{F}_{\text{life}} - 1|$, i.e., $\tilde{F}_{\text{life}} < 1$, or (27) may be infeasible hence no solution is possible. Instead, we let $\bar{S}_t = \bar{S}^{\text{P}} \in \mathbb{R}$ be constant $\forall t \in \mathcal{T}^{\text{P}}$, and we propose Algorithm 1 to search for an optimal value of \bar{S}^{P} , such that (a) the optimization problem (27) is feasible, and (b) $|\tilde{F}_{\text{life}} - 1|$ is minimized.

4.4 Search algorithm

In general, the search algorithm constructs sequences of upper bounds $\{u_n\}$ and lower bounds $\{l_n\}$. Candidate values of \bar{S}_n^{P} are evaluated between $\{u_n\}$ and $\{l_n\}$, and the search direction depends on the solution to (27) and the resulting $F_{\text{life},n}$ by applying the \bar{S}_n^{P} limit at iteration n .

To show that the sequence of \bar{S}_n^{P} converges to a limit \bar{S}_*^{P} , i.e., $\lim_{n \rightarrow \infty} \bar{S}_n^{\text{P}} = \bar{S}_*^{\text{P}}$, we first discuss monotonic properties of the sequences $\{u_n\}$ and $\{l_n\}$ constructed by the algorithm.

Algorithm 1 Search algorithm for optimal \bar{S}^P

```

Initialize
 $n \leftarrow 0$ 
 $u_n \leftarrow \max_t \{x_{t,e}(p^0)\}$ 
 $l_n \leftarrow 0$ 
 $\bar{S}_n^P \leftarrow \delta \ll u_n$ 
while  $u_n - l_n > \delta$  do
  Construct  $\bar{S}_t$  using  $\bar{S}_n^P$  and (30)
  Solve the optimization problem (27)
   $n \leftarrow n + 1$ 
  if a feasible solution is obtained then
    Compute the resulting loading and  $F_{\text{life},n}$  from ts-REM and TAM models, respectively
    if  $F_{\text{life},n} > 1$  then
       $\bar{S}_n^P \leftarrow \max\{l_{n-1}, \bar{S}_{n-1}^P \exp(-1/n)\}$ 
      if  $\bar{S}_n^P$  has already been tried then
         $\bar{S}_n^P \leftarrow \frac{(l_{n-1} + \bar{S}_{n-1}^P)}{2}$ 
      end if
       $u_n \leftarrow \bar{S}_{n-1}^P$ 
       $l_n \leftarrow l_{n-1}$ 
    else if  $F_{\text{life},n} \leq 1$  then
       $\bar{S}_n^P \leftarrow \min\{u_{n-1}, \bar{S}_{n-1}^P \exp(1/n)\}$ 
      if  $\bar{S}_n^P$  has already been tried then
         $\bar{S}_n^P \leftarrow \frac{(u_{n-1} + \bar{S}_{n-1}^P)}{2}$ 
      end if
       $l_n \leftarrow \bar{S}_{n-1}^P$ 
       $u_n \leftarrow u_{n-1}$ 
    end if
  else if no feasible solution is obtained then
     $\bar{S}_n^P \leftarrow \min\{u_{n-1}, \bar{S}_{n-1}^P \exp(1/n)\}$ 
    if  $\bar{S}_n^P$  has already been tried then
       $\bar{S}_n^P \leftarrow \frac{1}{2}(u_{n-1} + \bar{S}_{n-1}^P)$ 
    end if
     $l_n \leftarrow \bar{S}_{n-1}^P$ 
     $u_n \leftarrow u_{n-1}$ 
  end if
end while

```

Lemma 1. Consider Algorithm 1, the following statements hold for $n > 0$:

- (A) The sequence of upper bounds $\{u_n\}$ is monotonically non-increasing, and the sequence of lower bounds $\{l_n\}$ is monotonically non-decreasing.
- (B) At any $n > 0$, $u_n \geq l_n$.
- (C) $\lim_{n \rightarrow \infty} u_n = \inf\{u_n\}$, and $\lim_{n \rightarrow \infty} l_n = \sup\{l_n\}$.

Proof. For $n > 0$, we have the following two cases:

1. If a solution to (27) has been found at iteration $n - 1$, we can calculate the resulting $F_{\text{life},n}$ and

- (a) if $F_{\text{life},n} > 1$, then $\bar{S}_n^P \leq \bar{S}_{n-1}^P$, $u_n = \bar{S}_{n-1}^P$, and $l_n = l_{n-1}$. Further, as \bar{S}_n^P is bounded below by l_{n-1} , we also have $u_n = \bar{S}_{n-1}^P \geq \bar{S}_n^P \geq l_{n-1} = l_n$.

Applying \bar{S}_n^P at iteration n , we have the following three cases:

- i. if a solution to (27) is found and $F_{\text{life},n+1} > 1$, then $u_{n+1} = \bar{S}_n^P \leq \bar{S}_{n-1}^P = u_n$, and $l_{n+1} = l_n$.
- ii. if a solution to (27) is found but $F_{\text{life},n+1} \leq 1$, then $u_{n+1} = u_n$, and $l_{n+1} = \bar{S}_n^P \geq l_{n-1} = l_n$.
- iii. if no solution to (27) is found, then $u_{n+1} = u_n$, and $l_{n+1} = \bar{S}_n^P \geq l_{n-1} = l_n$.

Hence in cases a.(i)-(iii), we have $u_{n+1} \leq u_n$ and $l_{n+1} \geq l_n$.

- (b) if $F_{\text{life},n} \leq 1$, then $\bar{S}_n^P \geq \bar{S}_{n-1}^P$, $u_n = u_{n-1}$, and $l_n = \bar{S}_{n-1}^P$. Further, as \bar{S}_n^P is bounded above by u_{n-1} , we have $u_n = u_{n-1} \geq \bar{S}_n^P \geq \bar{S}_{n-1}^P = l_n$.

At the next iteration, we have the following three cases:

- i. if a solution to (27) is found and $F_{\text{life},n+1} > 1$, then $u_{n+1} = \bar{S}_n^P \leq u_{n-1} = u_n$ and $l_{n+1} = l_n$.
- ii. if a solution to (27) is found but $F_{\text{life},n+1} \leq 1$, then $u_{n+1} = u_n$ and $l_{n+1} = \bar{S}_n^P \geq \bar{S}_{n-1}^P = l_n$.
- iii. if no solution to (27) is found, then $u_{n+1} = u_n$, and $l_{n+1} = \bar{S}_n^P \geq \bar{S}_{n-1}^P = l_n$.

Hence in cases b.(i)-(iii), we have $u_{n+1} \leq u_n$ and $l_{n+1} \geq l_n$.

2. If there exists no solution to (27) at iteration $n-1$, then $\bar{S}_n^P \geq \bar{S}_{n-1}^P$, $u_n = u_{n-1}$, and $l_n = \bar{S}_{n-1}^P$. The same argument as in 1.b lead to $u_n \geq l_n$.

At the next iteration, by the same argument as in 1.b, we have $u_{n+1} \leq u_n$ and $l_{n+1} \geq l_n$.

In cases 1) and 2) we show that $u_{n+1} \leq u_n$ and $l_{n+1} \geq l_n$ hold, hence Lemma 1-(A) is proved. In addition, we also show that $u_n \geq l_n$ holds in these cases, hence Lemma 1-(B) is proved.

As $\{u_n\}$ is monotonically non-increasing and is bounded below by $\{l_n\}$, by the monotone convergence theorem, $\{u_n\}$ converges to its infimum. Similarly, $\{l_n\}$ converges to its supremum. Hence Lemma 1-(C) also holds. \square

Next, we argue that the candidate value \bar{S}_n^P at iteration n must differ from that at the previous iteration, except in the following special cases.

Lemma 2. For $n > 0$, the following statements hold for the \bar{S}_n^P computed by Algorithm 1:

- (A) If there exists a solution to (27) at iteration $n-1$ and $F_{\text{life},n} > 1$, then $\bar{S}_n^P = \bar{S}_{n-1}^P$ if and only if $\bar{S}_{n-1}^P = l_{n-1}$.
- (B) If there exists a solution to (27) at iteration $n-1$ and $F_{\text{life},n} \leq 1$ or (27) is infeasible at iteration $n-1$, then $\bar{S}_n^P = \bar{S}_{n-1}^P$ if and only if $\bar{S}_{n-1}^P = u_{n-1}$.

Proof. We start with Lemma 2-(A) and prove the statement in both directions.

(\Rightarrow) If $\bar{S}_{n-1}^P = l_{n-1}$, by the construction of Algorithm 1 we have $\bar{S}_n^P \geq l_{n-1}$ and $\bar{S}_n^P \leq \bar{S}_{n-1}^P = l_{n-1}$ at the same time. Therefore, $\bar{S}_n^P = l_{n-1} = \bar{S}_{n-1}^P$ must hold.

(\Leftarrow) If $\bar{S}_n^P = \bar{S}_{n-1}^P$, then \bar{S}_n^P can only take the following possible values by Algorithm 1:

- (a) $\bar{S}_n^P = l_{n-1}$, then $\bar{S}_n^P = \bar{S}_{n-1}^P = l_{n-1}$.
- (b) $\bar{S}_n^P = \frac{(l_{n-1} + \bar{S}_{n-1}^P)}{2}$, i.e., $\bar{S}_n^P = l_{n-1}$ has already been tried in previous iterations, then

$$\begin{aligned} 2\bar{S}_{n-1}^P &= l_{n-1} + \bar{S}_{n-1}^P \\ \Leftrightarrow \bar{S}_{n-1}^P &= l_{n-1}. \end{aligned}$$

Hence $\bar{S}_{n-1}^P = l_{n-1}$ always holds if $\bar{S}_n^P = \bar{S}_{n-1}^P$.

Therefore, it is shown that $\bar{S}_n^P = \bar{S}_{n-1}^P$ if and only if $\bar{S}_{n-1}^P = l_{n-1}$ when (27) is feasible and $F_{\text{life},n} > 1$.

The proof of Lemma 2-(B) follows the same argument as in Lemma 2-(A), and hence it is omitted. \square

By Lemma 1 we established that the sequences $\{u_n\}$ and $\{l_n\}$ are monotonic and convergent. We now show that they converge to the same limit.

Lemma 3. The sequences $\{u_n\}$ and $\{l_n\}$ constructed by Algorithm 1 converge to the same limit, i.e., $\lim_{n \rightarrow \infty} u_n = \lim_{n \rightarrow \infty} l_n$.

Proof. Suppose that at $n = N$, we have $u_N = u_*$, $l_N = l_*$. Let $\delta_N \triangleq u_N - l_N \geq 0$. If $\delta_N = 0$, then $u_* = l_*$. By Lemma 1 $\{u_n\}$ and $\{l_n\}$ are monotonic and $u_n \geq l_n$, $\forall n > 0$, then we must have $u_n = l_n = u_* = l_*$, $\forall n > N$. In this case, $\{u_n\}$ and $\{l_n\}$ converge to the same limit and the proof is done.

Now we consider $\delta_N > 0$. At the next iteration $n = N + 1$, the following cases may occur:

1. If there exists a solution to (27) at iteration N and $F_{\text{life}, N+1} > 1$, then we have shown in Lemma 1 that $\bar{S}_{N+1}^P \leq \bar{S}_N^P$, $u_{N+1} = \bar{S}_N^P$, and $l_{N+1} = l_N = l_*$. We thus have:

$$\begin{aligned} u_{N+1} - l_{N+1} &= \bar{S}_N^P - l_*, \\ &= (u_* - l_*) + (\bar{S}_N^P - u_*), \\ &= \delta_N + (\bar{S}_N^P - u_*). \end{aligned}$$

In what follows, we argue $u_{N+1} - l_{N+1} < \delta_N$ for any value of \bar{S}_{N+1}^P and \bar{S}_N^P :

- (a) When $\bar{S}_{N+1}^P = \bar{S}_N^P$, by Lemma 2-(A) we have $\bar{S}_N^P = l_N = l_*$. Hence,

$$\begin{aligned} u_{N+1} - l_{N+1} &= \delta_N + (\bar{S}_N^P - u_*), \\ &= \delta_N + (l_* - u_*), \\ &= \delta_N - \delta_N, \\ &= 0. \end{aligned}$$

- (b) When $\bar{S}_{N+1}^P < \bar{S}_N^P$, $u_{N+1} \leq u_N = u_*$ always holds by the monotonicity of $\{u_n\}$. As $F_{\text{life}, N+1} > 1$ is assumed, we have $u_{N+1} = \bar{S}_N^P$ which leads to $\bar{S}_N^P \leq u_*$. If $\bar{S}_N^P < u_*$, then $u_{N+1} - l_{N+1} < \delta_N$ must hold.

We now argue that $\bar{S}_N^P = u_*$ cannot happen. By the construction of Algorithm 1, u_N is updated to u_* as $\bar{S}_{n_u}^P$ reaches this value at some iteration $n_u < N$. When \bar{S}_N^P reaches u_* again at iteration N , it would need to be adjusted to $\bar{S}_N^P = \frac{(l_* + \bar{S}_{N-1}^P)}{2}$ according to the algorithm. We show by contradiction that the adjusted $\bar{S}_N^P \neq u_*$. Let us assume for now that the adjusted $\bar{S}_N^P = u_*$, we have:

$$\begin{aligned} 2\bar{S}_N^P &= l_* + \bar{S}_{N-1}^P \\ \Leftrightarrow 2u_* &= l_* + \bar{S}_{N-1}^P \\ \Leftrightarrow u_* + (u_* - l_*) &= \bar{S}_{N-1}^P \\ \Leftrightarrow u_* + \delta_N &= \bar{S}_{N-1}^P. \end{aligned} \tag{31}$$

As \bar{S}_{N-1}^P is bounded above by u_* and $\delta_N > 0$, (31) must not hold. Hence, by contradiction, $\bar{S}_N^P \neq u_*$ and we must have $\bar{S}_N^P < u_*$. In such a case,

$$u_{N+1} - l_{N+1} = \delta_{N+1} < \delta_N.$$

From cases a) and b), we establish that the sequence $\{u_n - l_n\}$ is monotonically decreasing and bounded below by 0. Hence by the monotone convergence theorem,

$$\lim_{n \rightarrow \infty} (u_n - l_n) = 0 \Leftrightarrow \lim_{n \rightarrow \infty} u_n = \lim_{n \rightarrow \infty} l_n.$$

2. By similar argument, we can arrive at $\lim_{n \rightarrow \infty} u_n = \lim_{n \rightarrow \infty} l_n$ when there exists a solution to (27) at iteration N and $F_{\text{life}, N+1} \leq 1$, or when no solution is found for (27) at iteration N . \square

Now we state the main result for the convergence of the sequence $\{\bar{S}_n^P\}$ constructed by the search algorithm.

Theorem 1. The sequences $\{\bar{S}_n^P\}$, $\{u_n\}$, and $\{l_n\}$ generated by Algorithm 1 for $n > 0$ converge to \bar{S}_*^P .

Proof. The sequence $\{\bar{S}_n^P\}$ is bounded by $\{u_n\}$ and $\{l_n\}$ for all n . By Lemma 3, we have $\lim_{n \rightarrow \infty} u_n = \lim_{n \rightarrow \infty} l_n$. By the squeeze theorem, it follows that $\lim_{n \rightarrow \infty} \bar{S}_n^P = \bar{S}_*^P = \lim_{n \rightarrow \infty} u_n = \lim_{n \rightarrow \infty} l_n$. \square

Let $\bar{S}_{t,*}$ be the \bar{S}_t computed in (30) for $t \in \mathcal{T}^{\text{OP}} \cup \mathcal{T}^{\text{MP}}$ and the searched \bar{S}_*^P for $t \in \mathcal{T}^P$. The following corollary can be consequently claimed.

Corollary 1. If $\tilde{F}_{\text{life}} = 1$ can be achieved, then \bar{S}_*^P is an optimal value to achieve $\tilde{F}_{\text{life}} = 1$. Further, (27) is a convex restriction of (22).

Proof. When applying $\bar{S}_{t,*}$, the resulting adjustment Δ_{prob} and incentives are (i) feasible with respect to the original problem (22), and (ii) globally optimal with respect to the convex problem (27). Given that $\tilde{F}_{\text{life}} = 1$, the relaxation of (14) is exact. It therefore follows that (27) is a convex restriction of (22). \square

If there exists no \bar{S}^P to achieve $\tilde{F}_{\text{life}} = 1$, Theorem 1 still holds and yields some $\bar{S}_{t,*}$ that minimizes $|\tilde{F}_{\text{life}} - 1|$. In this case, (27) is a convex approximation to (22). We can still solve for Δ_{prob} and incentives from (27), but the relaxation of (14) is not exact.

5 Numerical study

We use the modified IEEE-8500 test network as in [20] to illustrate the proposed strategies. We specifically aim to mitigate overloads on the substation transformer. The following information are assumed:

- \mathcal{L}_{EV} : charging may start at each hour and lasts for 2, 4, or 6 hours, and 4 levels of EV charging power are considered (1.8kW, 3.6kW, 6.6kW, 7.2kW, with unity power factor).
- $\text{Pr}_{\mathcal{L}}$: each customer's probability of adopting each profile in \mathcal{L}_{EV} is randomly generated without using any known distribution, but to be more realistic, customers have higher probabilities of starting charging between noon and midnight.
- The nominal electricity price is $p_{\text{rate}}^{\text{nom}} = 0.35$ \$/kWh. According to [16], the averaged elasticity factor $\bar{\varepsilon}$ ranges from -0.21 to -0.61 . Hence we assume $\bar{\varepsilon} = -0.4$.

We look at the impact to the substation transformer loading levels at 80% EV penetration for $\mathcal{T} = 24$ hours with a time step of $\Delta t = 1$ hour. Figure 1 shows the mean and maximum/minimum ($\pm 2 \times$ standard deviation) loading levels which are computed by the ts-REM model.

If we look at the mean loading curve (in orange color), the transformer is overloaded from 3PM until 10PM with the worst loading at around 125%. If such a loading pattern repeats during the entire year, it is determined by TAM that the lifetime factor is $F_{\text{life}} = 1.1$. Suppose that the annual cost of

the transformer at the nominal lifetime is $c_{\text{annual}} = \$500,000$, then from (13) an extra cost of \$50,000 per year is incurred to utilities due to the shortened lifetime, which serves as the budget for customer incentives.

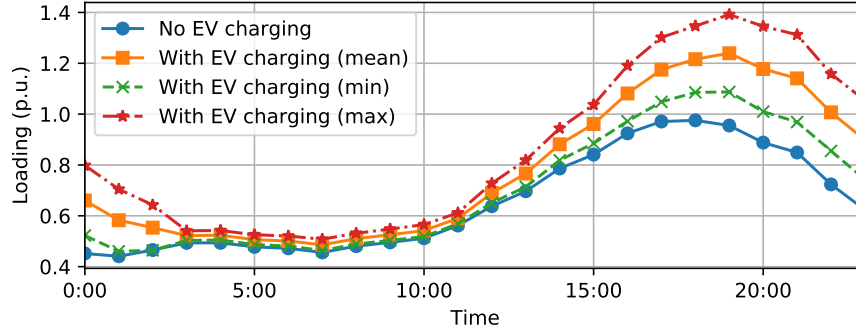


Figure 1: Multiple levels of loading curves of the substation transformer with 80% EV penetration

Based on the loading curves in Figure 1, we set \mathcal{T}^P and \mathcal{T}^{OP} to $[14:00, 21:00)$ and $[0:00, 6:00)$, respectively, and the remaining hours to \mathcal{T}^{MP} . Figure 2 shows the \bar{S}_n^P value searched at each iteration of Algorithm 1 for the reward type of incentives (top left) and for TOU pricing (top right). Figure 2 also shows the corresponding total yearly costs (bottom left) and the incentives levels of ξ and η (bottom right) of each iteration. For the reward incentives, \bar{S}_n^P converges to $\bar{S}_*^P = 0.61$, the unit reward is $r = 10.82$ ¢/kWh, and the total extra cost to utilities reduces from an initial \$50,000 to \$18,868 per year (a 62.3% saving). For the TOU pricing, \bar{S}_n^P converges to $\bar{S}_*^P = 0.66$, a discount of $\xi = 20.25$ ¢/kWh is offered during the off-peak time, and a surcharge of $\eta = 11.69$ ¢/kWh is added during the peak time. Under such pricing, the total extra cost to utilities reduces from \$50,000 to \$16,973 per year (a 66.1% saving). It is noted that the TOU program is slightly more efficient and the total cost to implementing the mitigation strategy is less.

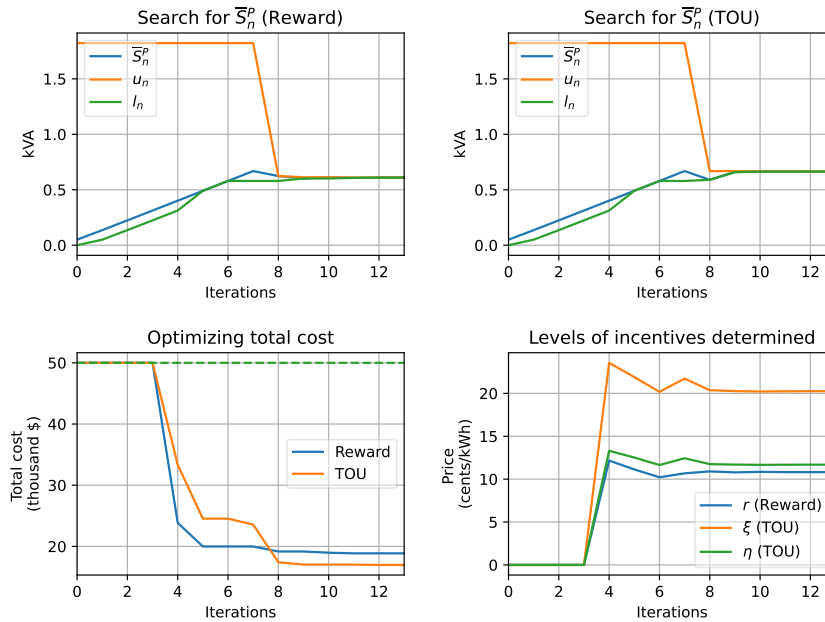


Figure 2: The sequences of \bar{S}_n^P searched (top), total costs (bottom left), and incentive levels of r, ξ, η (bottom right) during iterations of Algorithm 1

Figure 3 shows the results when the mitigation strategies based on the converged solutions for the two types of incentive programs are applied. The bottom chart compares the averaged probabilities of all customers charging EVs at different hours during the day. With the mitigation strategies applied, customers decrease their probabilities of charging EVs during the peak period and increase the probabilities during the off-peak period, while the probabilities of the mid-peak period remain unchanged. As a consequence, the transformer’s overload during the peak period has been reduced to an acceptable level while the loading during the off-peak period is increased as shown in the top and middle charts of Figure 3. Although the transformer is still slightly overloaded for a brief period, its lifetime of service is maintained at the nominal value under either type of incentive programs, i.e., $\tilde{F}_{life} = 1$.

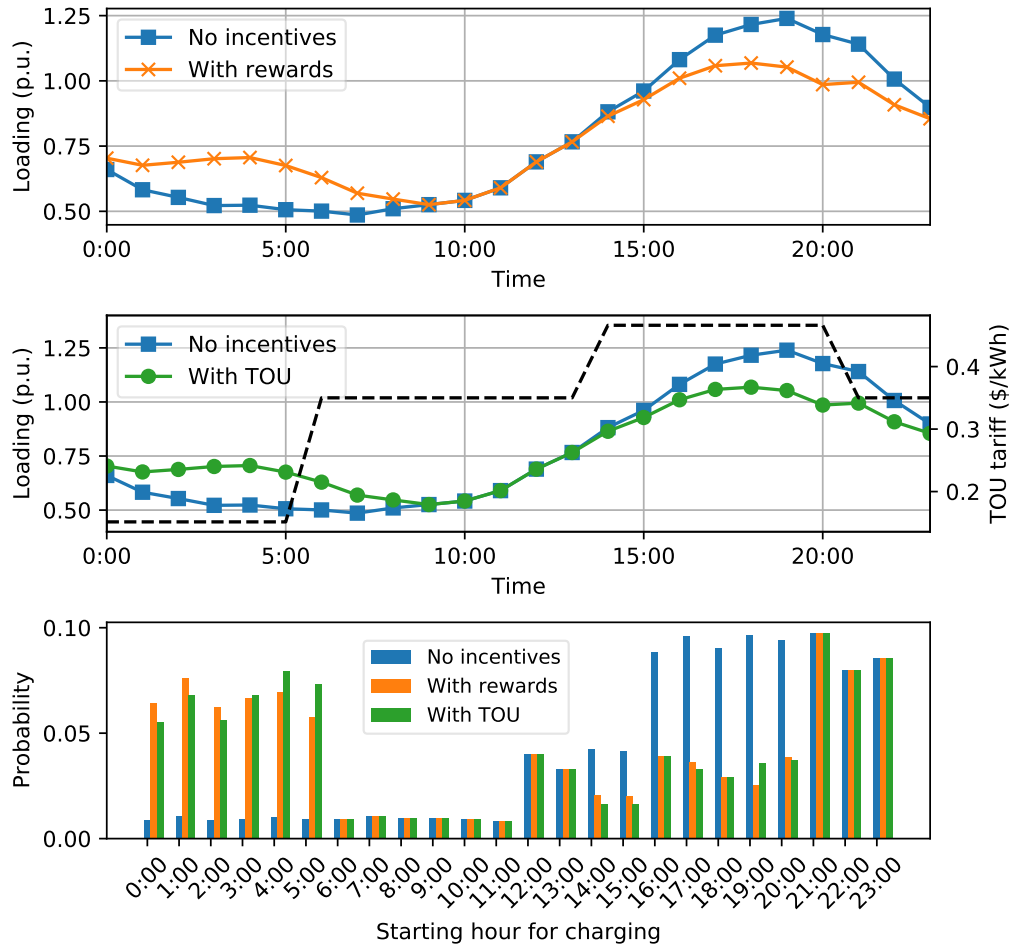


Figure 3: Mitigation of the substation transformer overload by offering rewards (top) or by applying TOU (middle) and the resulting changes to customers’ EV charging habits (probabilities of charging hours, bottom)

While all customers’ averaged probabilities of charging profiles are compared in Figure 3, Figure 4 shows the shifts of individual probabilities of 100 customers under the mitigation strategies. All customers had higher probabilities of charging their EVs during the peak period which overloads the transformer, and they increase the probabilities of charging during the off-peak period to receive the incentives offered under the mitigation strategies.

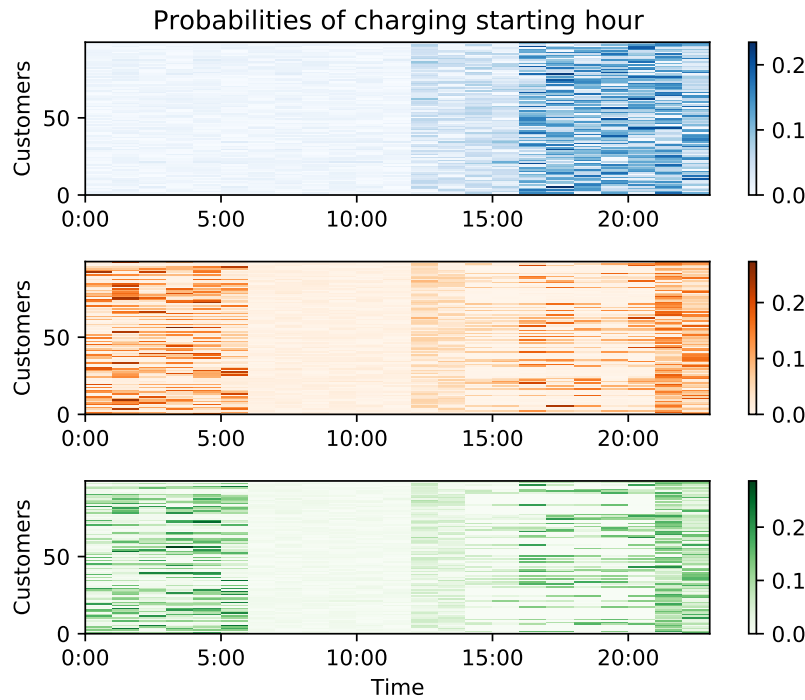


Figure 4: Comparison of 100 customers' probabilities of charging during the day before adopting a mitigation strategy (top) versus those by offering rewards (middle) or by applying TOU (bottom)

6 Conclusion

In this paper, we extended the rapid assessment method to perform a time-series impact analysis of EV charging on power distribution networks. We focus on the case where the analysis result indicates overloading issues to network equipment. To avoid loss of equipment's usable lifetime and to minimize associated costs, a mitigation strategy is designed to shift customers' probabilities of charging their EVs from peak hours to off-peak hours. Two types of incentive programs are considered, and a dedicated search algorithm embedded with a convex optimization problem is proposed to determine optimal levels of incentives. It is noted that under the proposed mitigation strategy, we do not enforce a specific charging schedule on a daily basis. Rather, customers are still allowed to charge their EVs during the peak hours when necessary. However, the probabilities of doing so in the long term should be consistent with those determined from the mitigation plan.

Although the numerical example presented considers the full participation of customers, our formulation can also account for the uncertainty in customers' participation through the λ_p factor. This offers the opportunity to perform various case studies with different participation rates and sensitivity analysis including validation studies with real customer data for utilities as a next step.

References

- [1] IEEE Std 1283-2013 (Revision of IEEE Std 1283-2004): IEEE Guide for Determining the Effects of High-Temperature Operation on Conductors, Connectors, and Accessories. IEEE.
- [2] IEEE guide for loading mineral-oil-immersed transformers and step-voltage regulators. IEEE Std C57.91-2011 (Revision of IEEE Std C57.91-1995), pages 1–123, 2012.
- [3] Muhammad Ashfaq, Osama Butt, Jeyraj Selvaraj, and Nasrudin Rahim. Assessment of electric vehicle charging infrastructure and its impact on the electric grid: A review. *International Journal of Green Energy*, 18(7):657–686, 2021.

- [4] Mohamed A Awadallah, Birendra N Singh, and Bala Venkatesh. Impact of ev charger load on distribution network capacity: A case study in toronto. *Canadian Journal of Electrical and Computer Engineering*, 39(4):268–273, 2016.
- [5] Yijia Cao, Shengwei Tang, Canbing Li, Peng Zhang, Yi Tan, Zhikun Zhang, and Junxiong Li. An optimized EV charging model considering TOU price and SOC curve. *IEEE Transactions on Smart Grid*, 3(1):388–393, 2012.
- [6] Sanya Carley, Rachel M Krause, Bradley W Lane, and John D Graham. Intent to purchase a plug-in electric vehicle: A survey of early impressions in large US cities. *Transportation Research Part D: Transport and Environment*, 18:39–45, 2013.
- [7] Kristien Clement-Nyns, Edwin Haesen, and Johan Driesen. The impact of charging plug-in hybrid electric vehicles on a residential distribution grid. *IEEE Transactions on Power Systems*, 25(1):371–380, 2010.
- [8] Illia Diahovchenko, Roman Petrichenko, Lubov Petrichenko, Anatolijs Mahnitko, Pavlo Korzh, Michal Kolcun, and Zsolt Čonka. Mitigation of transformers’ loss of life in power distribution networks with high penetration of electric vehicles. *Results in Engineering*, 15:100592, 2022.
- [9] Weihui Fu, James D McCalley, and Vijay Vittal. Risk assessment for transformer loading. *IEEE Transactions on Power Systems*, 16(3):346–353, 2001.
- [10] Pacific Gas and Electric Company (PG&E). Electric Vehicle (EV) rate plans – (EV-B) rate. https://www.pge.com/en_US/residential/rate-plans/rate-plan-options/electric-vehicle-base-plan/electric-vehicle-base-plan.page?
- [11] Neeraj Gupta. Probabilistic optimal reactive power planning with onshore and offshore wind generation, ev, and pv uncertainties. *IEEE Transactions on Industry Applications*, 56(4):4200–4213, 2020.
- [12] Salman Habib, Muhammad Mansoor Khan, Farukh Abbas, Muhammad Numan, Yaqoob Ali, Houjun Tang, and Xuhui Yan. A framework for stochastic estimation of electric vehicle charging behavior for risk assessment of distribution networks. *Frontiers in Energy*, 14(2):298–317, 2020.
- [13] Salman Habib, Muhammad Mansoor Khan, Farukh Abbas, Muhammad Numan, Yaqoob Ali, Houjun Tang, and Xuhui Yan. A framework for stochastic estimation of electric vehicle charging behavior for risk assessment of distribution networks. *Frontiers in Energy*, 14(2):298–317, 2020.
- [14] Salman Habib, Muhammad Mansoor Khan, Farukh Abbas, Lei Sang, Muhammad Umair Shahid, and Houjun Tang. A comprehensive study of implemented international standards, technical challenges, impacts and prospects for electric vehicles. *IEEE Access*, 6:13866–13890, 2018.
- [15] D.S. Kirschen, G. Strbac, P. Cumperayot, and D. de Paiva Mendes. Factoring the elasticity of demand in electricity prices. *IEEE Transactions on Power Systems*, 15(2):612–617, 2000.
- [16] Xavier Labandeira, José M Labeaga, and Xiral López-Otero. A meta-analysis on the price elasticity of energy demand. *Energy policy*, 102:549–568, 2017.
- [17] Rong-Ceng Leou, Chun-Lien Su, and Chan-Nan Lu. Stochastic analyses of electric vehicle charging impacts on distribution network. *IEEE Transactions on Power Systems*, 29(3):1055–1063, 2014.
- [18] Randall J LeVeque. *Finite volume methods for hyperbolic problems*, volume 31. Cambridge university press, 2002.
- [19] F Li, I Kocar, and A Lesage-Landry. Mitigating equipment overloads due to electric vehicle charging using customer incentives. In *2023 IEEE Power & Energy Society General Meeting (PESGM)*, 2023.
- [20] Feng Li, Ilhan Kocar, and Antoine Lesage-Landry. A rapid method for impact analysis of grid-edge technologies on power distribution networks. *IEEE Transactions on Power Systems*, pages 1–12, 2023.
- [21] Sichen Li, Weihao Hu, Di Cao, Zhenyuan Zhang, Qi Huang, Zhe Chen, and Frede Blaabjerg. A multiagent deep reinforcement learning based approach for the optimization of transformer life using coordinated electric vehicles. *IEEE Transactions on Industrial Informatics*, 18(11):7639–7652, 2022.
- [22] Sohaib Rafique, Mohammad Sohrab Hasan Nizami, Usama Bin Irshad, Mohammad Jahangir Hossain, and Subhas Chandra Mukhopadhyay. EV scheduling framework for peak demand management in LV residential networks. *IEEE Systems Journal*, 16(1):1520–1528, 2021.
- [23] Jukka Saarenpää, Mikko Kolehmainen, and Harri Niska. Geodemographic analysis and estimation of early plug-in hybrid electric vehicle adoption. *Applied Energy*, 107:456–464, 2013.
- [24] Shengnan Shao, Manisa Pipattanasomporn, and Saifur Rahman. Grid integration of electric vehicles and demand response with customer choice. *IEEE Transactions on Smart Grid*, 3(1):543–550, 2012.
- [25] Shengnan Shao, Tianshu Zhang, Manisa Pipattanasomporn, and Saifur Rahman. Impact of TOU rates on distribution load shapes in a smart grid with PHEV penetration. In *IEEE PES T&D 2010*, pages 1–6, 2010.

-
- [26] Eric Sortomme, Mohammad M. Hindi, S. D. James MacPherson, and S. S. Venkata. Coordinated charging of plug-in hybrid electric vehicles to minimize distribution system losses. *IEEE Transactions on Smart Grid*, 2(1):198–205, 2011.
 - [27] Gil Tal, Debapriya Chakraborty, Alan Jenn, Jae Hyun Lee, and David Bunch. Factors affecting demand for plug-in charging infrastructure: An analysis of plug-in electric vehicle commuters. UC Office of the President: University of California Institute of Transportation Studies, 2020.
 - [28] Michael A Tamor, Chris Gearhart, and Ciro Soto. A statistical approach to estimating acceptance of electric vehicles and electrification of personal transportation. *Transportation Research Part C: Emerging Technologies*, 26:125–134, 2013.